



## Identification of amidoheteroaryls as potent inhibitors of mutant (V600E) B-Raf kinase with in vivo activity

Paul D. Lyne\*, Brian Aquila, Donald J. Cook, Les A. Dakin, Jay Ezhuthachan, Stephanos Ioannidis, Timothy Pontz, Mei Su, Qing Ye, Xiaolan Zheng, Michael H. Block, Scott Cowen, Tracy L. Deegan, John W. Lee, David A. Scott, Dominique Custeau, Lisa Drew, Srinivasu Poondru, Minhui Shen, Allan Wu

Cancer Research, AstraZeneca R&D Boston, 35 Gatehouse Drive, Waltham, MA 02451, USA

### ARTICLE INFO

#### Article history:

Received 3 September 2008

Revised 7 October 2008

Accepted 10 October 2008

Available online 15 October 2008

#### Keywords:

B-Raf

V600E

Amidoheteroaryl

### ABSTRACT

A series of amidoheteroaryl compounds were designed and synthesized as inhibitors of B-Raf kinase. Several compounds from the series show excellent potency in biochemical, phenotypic and mode of action cellular assays. Potent examples from the series have also demonstrated good plasma exposure following an oral dose in rodents and activity against the Ras-Raf pathway in tumor bearing mice.

© 2008 Elsevier Ltd. All rights reserved.

B-Raf is a member of the MAPK signaling cascade, sitting downstream of Ras. During MAPK signaling B-Raf phosphorylates its substrates Mek-1/2, which in turn phosphorylate Erk-1/2. Once phosphorylated the Erks translocate to the nucleus where they engage a number of transcription factors that ultimately leads to several biological responses including proliferation.<sup>1</sup> The Ras-Raf-Erk pathway has been implicated previously to play a role in oncogenesis having been demonstrated to promote proliferation, angiogenesis and survival in several cancer models.<sup>2</sup> Mutant forms of the kinase domain of B-Raf have been identified in a number of human cancer types, with the highest prevalence found in malignant melanoma tumors.<sup>3,4</sup> The most common mutation, the V600E mutant (<sup>m</sup>B-Raf), has been demonstrated in vitro to be constitutively active in carcinoma cells and to simulate the growth of cancer cells independent of upstream signaling. Based on this epidemiological data, inhibition of the kinase domain of B-Raf represents a promising strategy for the clinical treatment of cancers bearing the V600E mutation.

A subset of the AstraZeneca collection, known or expected to possess activity against kinases, including compounds screened previously against C-Raf,<sup>5</sup> was screened against <sup>m</sup>B-Raf and several series with good activity were identified. One of the promising hit series in terms of biochemical (enzyme) and cellular potency is shown in Figure 1 (**1**: enzyme IC<sub>50</sub> 0.002 μM; GI<sub>50</sub> (Colo205 cells) 5.9 μM; P-Erk (Colo205 cells) IC<sub>50</sub> 0.64 μM).

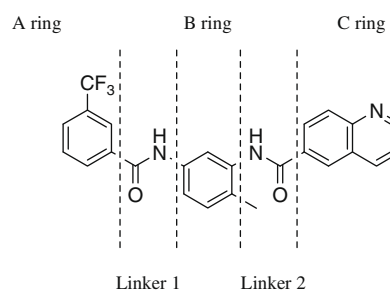
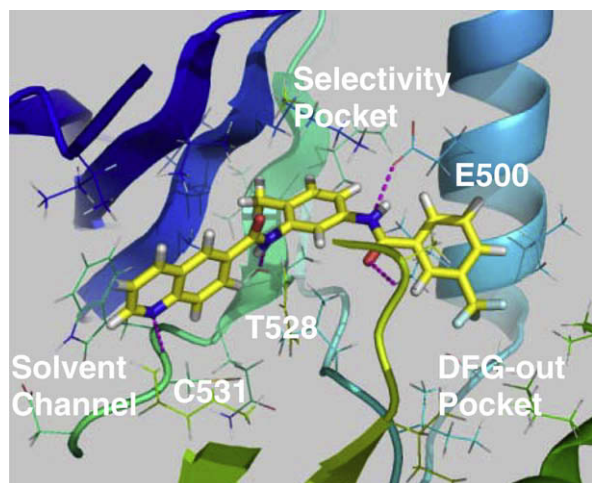


Figure 1. Bisamidophenyl screening hit **1**.

Modeling<sup>6</sup> of the initial hit **1** to the X-ray structure of <sup>m</sup>B-Raf (pdb code 1uwj<sup>7</sup>) suggested that this series bound to <sup>m</sup>B-Raf in a DFG-out<sup>8</sup> manner, with the quinoline located in the region of the hinge (Fig. 2). Preliminary efforts to explore the SAR of this series focused on replacement of the quinoline ring. Initial changes to the quinoline focused on changing the location of the aryl nitrogen and reduction in ring size to optimize the interaction between the Cys531 backbone NH and the inhibitor. As shown in Table 1, the potency of the series is sensitive to the location of the aryl nitrogen, and interestingly, monocyclic heteroaryl rings (**5**) were tolerated. This reduction in the molecular weight of the series was seen as advantageous for improving the physical properties. 3-Pyridyl analogs were most potent in the enzyme among the monocyclics. Furthermore, a significant increase in enzymatic and cellular potency was obtained by reversing the amide (in linker 2, **10**), which

\* Corresponding author.

E-mail address: [paul.lyne@astrazeneca.com](mailto:paul.lyne@astrazeneca.com) (P.D. Lyne).



**Figure 2.** Compound **1** docked into the binding site of V600E B-Raf (pdb code 1uwj). The quinoline makes a hydrogen bond to the backbone of Cys531. The amide between the B and C rings interacts with the gatekeeper Thr528. The amide between the A and B rings contributes to the stabilization of the DFG-out conformation of the protein with the trifluoromethylphenyl group buried in the induced pocket.

**Table 1**  
<sup>m</sup>B-Raf enzyme and cell P-Erk inhibition SAR for quinoline analogs.

Compound	X	IC <sub>50</sub> (μM) <sup>9</sup> <sup>m</sup> B-Raf	Cell (μM) <sup>10</sup> P-Erk IC <sub>50</sub>
1		0.002	0.64
2		0.005	0.73
3		10.5	—
4		0.001	0.40
5		0.049	>30
6		21.1	—
7		0.580	—
8		1.2	—
9		0.625	—
10		0.007	1.4

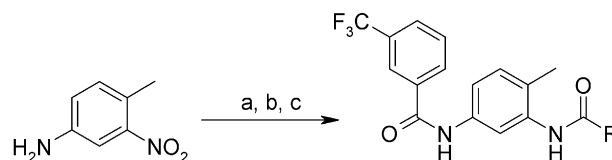
was attributed to an improvement in the interaction between the amide and the gatekeeper Thr528, and an improvement in the hydrogen bond accepting ability of the pyridyl nitrogen.

Compounds **1–9** were prepared via the route shown in Scheme 1. The strategy was to couple 3-(trifluoromethyl)benzoyl chloride with 4-methyl-3-nitroaniline followed by reduction with SnCl<sub>2</sub> to provide a key intermediate (92% yield for two steps) to examine multiple C rings.

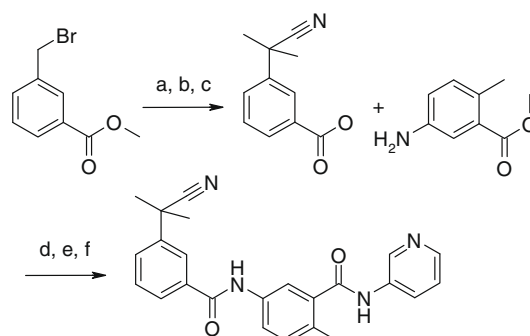
Subsequent optimization of **10** focused on the generation of an A-ring library to explore the SAR of the series in the DFG-out pocket. A variety of substituents on the 3-position of the A ring were found to yield compounds with potent inhibition in the enzyme assay. Similarly substituents at the 4-, 3,4-, and 3,5-positions also yielded potent compounds in the enzyme assay. A variety of substituents yielded excellent enzymatic potency, with substitution at the 3-position giving good cellular potency (inhibition of P-Erk levels), and in particular, the dimethylcyano group (**19**) resulted in a compound with the best cellular potency. Although compound **19** was found to have reasonable physical and pharmacokinetic properties, the clearance and bioavailability precluded testing of this compound in pharmacological assays (Table 3).

Compounds **10–25** were prepared via the route shown in Scheme 2. The dimethylcyano A ring was prepared by reacting methyl-3-(bromomethyl)benzoate with NaCN and then methyl iodide. Hydrolysis of the ester with LiOH provided the key A ring in a 43% overall yield. Coupling with methyl 5-amino-2-methylbenzoate followed by hydrolysis (98% yield for two steps) generated the acid that allowed extensive investigation of the C ring. Compound **19** was completed by coupling the A–B intermediate to pyridin-3-amine with HATU in DMF (98%). Ref. 11 provides detailed experiments for all analogs described in Tables 2 and 3.

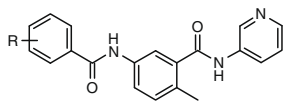
Optimization efforts for compound **19** focused on exploring substitution on the pyridyl C ring with a view to adding potency, blocking metabolic sites and adding steric hindrance to mitigate any potential for Cyp P450 inhibition (**10** Cyp2C9 IC<sub>50</sub> = 5 μM). In addition, based on structural information, a focused exploration of the B ring was examined. The ortho methyl group of the B ring



**Scheme 1.** Preparation of examples **1–9**. Reagents and conditions: (a) 3-(trifluoromethyl)benzoyl chloride, Et<sub>3</sub>N, DCM; (b) SnCl<sub>2</sub>·H<sub>2</sub>O, DMF; (c) RCO<sub>2</sub>H, HATU, *i*-Pr<sub>2</sub>NEt, DMF.



**Scheme 2.** Preparation of reversed amide examples. Reagents and conditions: (a) NaCN, DMF, 75 °C; (b) MeI, NaH, DMSO; (c) LiOH, THF/MeOH/H<sub>2</sub>O (3:1:1); (d) HATU, *i*-Pr<sub>2</sub>NEt, DMF; (e) LiOH, THF/MeOH/H<sub>2</sub>O (3:1:1); (f) Pyridin-3-amine, HATU, *i*-Pr<sub>2</sub>NEt, DMF.

**Table 2**  
SAR (biochemical and cellular) of the A ring.

Compound	R	IC <sub>50</sub> (μM) <sup>m</sup> B-Raf	Cell (μM) P-Erk IC <sub>50</sub>
11	3-CF <sub>3</sub>	0.007	1.4
12	3-F	0.322	—
13	3-Me	0.016	>30
14	3- <sup>i</sup> Pr	0.015	5.9
15	3-NMe <sub>2</sub>	0.016	14.6
16	3-Cl	0.012	>30
17	3-O <sup>i</sup> Pr	0.015	14.9
18	3-O <sup>t</sup> Bu	0.028	10.1
19	3-C(Me <sub>2</sub> )CN	0.007	0.33
20	3-CN	0.237	>30
21	3-SO <sub>2</sub> Me	0.011	>30
22	3-SO <sub>2</sub> NH <sub>2</sub>	0.030	>30
23	4-OMe	0.115	>30
24	3-CF <sub>3</sub> , 4-Cl	0.009	3.1
25	3-C(Me <sub>2</sub> )CN, 5-CNMe <sub>2</sub>	0.076	—

could be replaced with chloro and that change resulted in reduced metabolism without impacting cellular potency. The data for selected analogs are summarized in Table 3.

Substitution at the 2- and 3-positions of the pyridyl C ring led to improvements in cellular potency and in some cases to improved pharmacokinetic profiles. Addition of a hydrogen bond donor at the 2-position of the pyridyl ring resulted in good cellular potency with excellent potency seen for the acetamide analog **31**. Unfortunately, the metabolic lability and poor oral exposure of **31** prevented further progression. Attempts to introduce ionizable basic groups at the 2-position of the pyridyl ring generally increased solubility but resulted in decreases in cellular potency. A variety of groups with a range of electronic properties was tolerated at the 3-position. Introduction of a chloro group was found to be particularly beneficial for cellular potency. The P450 inhibition profile

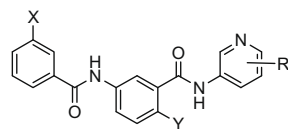
of the compounds did not seem to be alleviated by substitution on the pyridyl ring, with Cyp2C9 being consistently inhibited, albeit generally at low μM concentrations. Analogs that combined the best groups at both the 2- and 3-positions yielded compounds with excellent cellular potency and acceptable pharmacokinetic profiles.

The kinase selectivity profile of this series was assessed, using **39** as a representative. The dose response data are shown in Table 4. Within this panel, which includes a range of tyrosine and serine/threonine targets of therapeutic relevance, **39** was found to demonstrate good selectivity over the majority of the targets. Notable exceptions are the potent inhibitions of p38α and CSF-1R. The p38α activity is not surprising given a previous report of p38α activity for related compounds,<sup>14</sup> and data on a related series has been reported recently for CSF-1R.<sup>15</sup>

Based on the known MAPK pathway biology these particular off-target activities are not expected to contribute to inhibition

**Table 4**  
IC<sub>50</sub> data for **39** against a panel of kinases screened at K<sub>M</sub> for ATP in each case.

Kinase	IC <sub>50</sub> (μM)
p38α	0.005
CSF-1R	0.005
PDGFRβ	0.031
PTK2	0.478
EphB4	0.672
FGFR1	13.0
Jak2	29.0
Kdr	>30
EGFR	>30
IGFR1	>30
Pak1	>30
Plk	>30
Csk	>30
Src	>30
Chk-1	>30
Cdk2	>30
Jnk1	>30
PKA	>30

**Table 3**  
Enzyme and cellular potency, physical property data and rat PK upon iv (3 mpk) and po (10 mpk) dosing.<sup>13</sup>

Compound	R	X	Y	IC <sub>50</sub> (μM)	Cell (μM) P-Erk IC <sub>50</sub>	GI <sub>50</sub> <sup>12</sup> (μM)	Sol (μM) pH	Cyp2C9IC <sub>50</sub> (μM)	Cl (mL/min/kg)	T <sub>1/2</sub> (h)	V <sub>dss</sub> (L/kg)	F (%)
19	—	C(Me <sub>2</sub> )CN	Me	0.007	0.33	1.2	29		42.5	1.6	2.5	17
26	2-NH <sub>2</sub>	C(Me <sub>2</sub> )CN	Me	0.014	0.20	0.56			75.5	0.6	2.3	
27	2-Me	C(Me <sub>2</sub> )CN	Me	0.048	0.25	1.58	36	9.8	47.5	0.8	2.9	73
28	2-OMe	C(Me <sub>2</sub> )CN	Me	0.116	>30		13					
29	2-NMe	C(Me <sub>2</sub> )CN	Me	0.038	0.19	2.9		4.9	53.5	0.6	1.7	15
30	2-Morpholine	C(Me <sub>2</sub> )CN	Me	0.079	6.0		26					
31	2-NCCN(Me) <sub>2</sub>	C(Me <sub>2</sub> )CN	Me	0.048	1.4							
32	2-NCOMe	C(Me <sub>2</sub> )CN	Me	0.016	0.01	0.20	35		64	0.7	2.7	10
33	2-CN	C(Me <sub>2</sub> )CN	Me	0.205	>30		2					
34	3-Me	C(Me <sub>2</sub> )CN	Me	0.016	0.23	0.83	23	1.8	32.5	0.8	1.4	4
35	3-Cl	C(Me <sub>2</sub> )CN	Me	0.035	0.04	0.46	9	0.4	60	0.9	3.1	45
36	3-CONMe	C(Me <sub>2</sub> )CN	Me	0.017	0.89	2.1	21					
37	3-OMe	C(Me <sub>2</sub> )CN	Me	0.014	0.08	0.81	24		56	0.5	1.7	
38	2-NH <sub>2</sub> , 3-Cl	C(Me <sub>2</sub> )CN	Me	0.016	0.04	0.35	12	4.0	9.5	1.0	0.8	30
39	2-NH <sub>2</sub> , 3-Cl	CF <sub>3</sub>	Cl	0.027	0.08	0.86	<1	0.7	11	1.4	1.2	96
40	2-NH <sub>2</sub> , 3-Cl	CF <sub>3</sub>	Me	0.012	0.11	0.38	<1	1.8	8	1.6	1.0	78

**Table 5**

Pharmacodynamic data following a single oral dose to A375 tumor bearing Nude mice.

Compound	30 mpk	60 mpk	100 mpk
<i>P</i> -Erk Inhib. (%) 2 h post-dose			
<b>38</b>	0	40	83
<b>39</b>	50	64	71
<b>40</b>	18	67	81

of <sup>125</sup>I-Raf mediated signaling. The compound, **39**, was found to be inactive against Kdr and Cdks, which should aid in the interpretation of biological activity in future efficacy studies with this series.

Based on these optimization efforts compounds **38–40** were chosen for profiling in pharmacodynamic models. Each compound was dosed orally to A375 tumor (average tumor volume 200 mm<sup>3</sup>) bearing Nude mice. The mice were sacrificed and tumors were collected at specific timepoints post-dose. The tumors were lysed and analyzed for P-Erk levels. The activities of these compounds relative to vehicle control are shown in Table 5. Each of these compounds was able to inhibit the Raf-Mek-Erk pathway in tumors in a dose dependent manner.

In conclusion, amidoheteroaryl compounds presented here are potent inhibitors of mutant (V600E) B-Raf protein, which results in blockade of signaling through the Raf-Mek-Erk pathway in Colo205 cells in vitro, and in A375 tumor cells in vivo. Selected members of this series have pharmacokinetic properties that render them suitable for testing in cancer disease models and the results of such studies will be reported in due course.

## References and notes

- Peyssonnaud, C.; Eychene, A. *Biol. Cell* **2001**, *93*, 53.
- Dhomen, N.; Marais, R. *Curr. Opin. Genet. Dev.* **2007**, *17*, 31.
- Davies, H.; Bignell, G. R.; Cox, C.; Stephens, P.; Edkins, S., et al *Nature* **2002**, *417*, 949.
- Garnett, M. J.; Marais, R. *Cancer Cell* **2004**, *6*, 313.
- Hall-Jackson, C. A.; Evers, P. A.; Cohen, P.; Goedert, M.; Boyle, T. F., et al *Chem. Biol.* **1999**, *6*, 559.
- Docking was performed using Glide from the Schrodinger software suite (<http://www.schrodinger.com>). The ligand was built and refined using ligprep. The protein was prepared using pprep and the ligand was docked to the kinase domain using SP mode.
- Wan, P. T.; Garnett, M. J.; Roe, S. M.; Lee, S.; Niculescu-Duvaz, D.; Good, V. M.; Jones, C. M.; Marshall, C. J.; Springer, C. J.; Barford, D.; Marais, R. *Cell* **2004**, *116*, 855.
- (a) Pargellis, C.; Tong, L.; Churchill, L.; Cirillo, P. F.; Gilmore, T., et al *Nat. Struct. Biol.* **2002**, *9*, 268; (b) Mol, C. D.; Fabbro, D.; Horsfield, D. J. *Curr. Opin. Drug Discov. Dev.* **2004**, *7*, 639; (c) Knight, Z. A.; Shokat, K. M. *Chem. Biol.* **2005**, *12*, 621; (d) Liu, Y.; Gray, N. S. *Nat. Chem. Biol.* **2006**, *2*, 358.
- Activity of purified full length His-tagged human <sup>125</sup>I-Raf was determined in vitro using an Amplified Luminescent Proximity Homogeneous Assay (ALPHA) (Perkin-Elmer, MA). <sup>125</sup>I-Raf was expressed in insect cells and affinity purified by Ni<sup>2+</sup> agarose followed by Q-Sepharose chromatography. <sup>125</sup>I-Raf enzyme (0.12 nM), 84 nM biotinylated His-MEK1-AVI, and 24 μM ATP in 1.2× buffer was preincubated with compound for 20 min at 25 °C. Reactions were initiated with 24 mM MgCl<sub>2</sub> in 1.2× buffer and incubated at 25 °C for 60 min and reactions were stopped by addition of detection mix consisting of 20 mM Hepes, 102 mM ethylenediamine tetraacetic acid, 1.65 mg/mL BSA, 136 mM NaCl, 3.4 nM Phospho-MEK1/2 (Ser217/221) antibody (Cell Signaling Technology, Danvers, MA), 40 μg/mL Streptavidin donor beads (Perkin-Elmer, Waltham, MA), and 40 μg/mL Protein A acceptor beads (Perkin-Elmer, Waltham, MA). Plates were incubated at 25 °C for 18 h in the dark. Phosphorylated substrate was detected by an EnVision plate reader (Perkin-Elmer, Waltham, MA) 680 nm excitation, 520–620 nm emission. Data was graphed using Excel and IC<sub>50</sub>s determined.
- Cells were seeded into 96-well microplates (Costar, Corning, Lowell, MA) at 2 × 10<sup>5</sup> cells/well in phenol red free DMEM (Invitrogen, Carlsbad, CA) supplemented with 10% FBS. After 48 h, the cells were treated with DMSO or multiple concentrations of compound and then returned to the incubator for 75 min. Medium was then aspirated and cells fixed with a 6% formaldehyde solution for 20 min at room temperature. Cells were washed once with PBS containing 0.5% Triton X-100 (PBST) and 0.6% hydrogen peroxide added for 20 min at room temperature. After washing again in PBST, cells were blocked with 10% FBS/PBST solution for 1 h at room temperature. After washing, phospho-p44/42 monoclonal antibody (Cell Signaling Technology, Danvers, MA) was added and plates placed at 4 °C overnight. Plates were then washed in PBST, incubated with goat anti-mouse HRP-conjugated secondary antibody (Cell Signaling Technology, Danvers, MA) for 2 h at room temperature, washed in PBST, ABTS solution (Sigma, St. Louis, MO) added and plates incubated for 2 h at 30 °C. Quantification of signal was determined at OD405 using a SpectraMax plate reader (Molecular Devices, Sunnyvale, CA). Plates were then washed twice in PBST and twice in water. Crystal violet was then added and plates incubated for 20 min at room temperature. Washing was then repeated, 1% SDS solution with plates incubated with shaking for 20 min at room temperature. Quantification of signal was determined at OD595 using a SpectraMax plate reader (Molecular Devices, Sunnyvale, CA). Data was graphed using Excel and EC<sub>50</sub>s calculated.
- Pyridine carboxamide derivatives for use as anticancer agents*: Almeida, L.; Aquila, B.; Cook, D.; Cowen, S.; Dakin, L.; Ezhuthachan, J.; Ioannidis, S.; Lee, J. W.; Lee, S.; Lyne, P. D.; Pontz, T.; Scott, D.; Su, M.; Zheng, X. AstraZeneca AB, AstraZeneca UK Ltd, WO2006067446 A1, 2006.
- Cells were seeded into 96-well microplates (Costar, Corning, Lowell, MA) in phenol red-free RPMI DMEM (Invitrogen, Carlsbad, CA) supplemented with 10% FBS. Cell density was predetermined for each cell line based on linear phase growth over a 96 hour period. After overnight incubation, the cells were treated with DMSO or multiple concentrations of compound (day 0), and then returned to the incubator for 72 h (day 3). The number of viable cells on days 0 and 3 was determined using the CellTiter 96 Aqueous One Cell Proliferation Assay (Promega, Madison, WI). Quantification of signal was determined using a SpectraMax plate reader (Molecular Devices, Sunnyvale, CA). Percentage of net growth at day 3 (100%) relative to day 0 (0%) was calculated and the concentration of compound required to inhibit growth by 50% (GI50) determined.
- Compounds were administered to Han Wistar male rats in DMA/PEG/saline (40/40/20) solutions (iv dose) and (0.1%) HPMC suspensions (po dose).
- Brown, D. S.; Belfield, A. J.; Brown, G. R.; Campbell, D.; Foubister, A., et al *Bioorg. Med. Chem. Lett.* **2004**, *14*, 5383.
- Scott, D. A.; Aquila, B. M.; Beberitz, G. A.; Cook, D. J.; Dakin, L. A., et al *Bioorg. Med. Chem. Lett.* **2008**, *18*, 4794.